EUROPHYSICS LETTERS 15 February 1991

Europhys. Lett., 14 (4), pp. 331-336 (1991)

Convective *vs.* Absolute Instability in Couette-Taylor Flow with an Axial Flow.

A. TSAMERET and V. STEINBERG

Department of Nuclear Physics, Weizmann Institute of Science 76100 Rehovot, Israel

(received 9 October 1990; accepted in final form 6 December 1990)

PACS. 47.20 – Hydrodynamic stability and instability.
PACS. 47.60 – Flows in ducts, channels, and conduits (inc. Poiseuille and capillary flow).

Abstract. – Couette-Taylor flow between cylinders with a superimposed axial flow is studied experimentally. The axial flow suppresses the basic stationary instability and leads to propagating Taylor vortices through a forward oscillatory bifurcation. While the throughflow velocity increases the propagating vortices are pushed downstream to the outlet so that at the velocity which corresponds to the absolute instability limit, the pattern is «blown» out of the system. The surprising coexistence of steady Ekman and propagating Taylor vortices close to the inlet and outlet boundaries was discovered. The wave number selection mechanism, similar to that existing in the front-propagating case, is also identified.

The relation between convective and absolute stability conditions and the pattern selection problem was the subject of an interesting and intensive research on open and closed flow systems in recent years [1]. The distinction between convective and absolute instability conditions is well known in hydrodynamics [2], and in the framework of a Ginzburg-Landau (GL) equation for infinite and semi-infinite systems was discussed on several occasions [1, 3]. In the context of the GL equation it was shown [1, 3] that the transition between the two regimes occurs at some critical value of the group velocity S^* which is equal to the front propagation velocity in an infinite system [3].

However, in a finite geometry the sidewall reflection stabilizes the convective nature of propagating flows, as the theory [4] and the experiments [5] convincingly show that in a finite container absolute and convective instabilities lead to very different patterns. In the convective instability regime, travelling waves (TW) are localized. In the absolute instability regime one finds a saturated TW extending the entire cell besides the vicinity of the sidewall where TW are initiated. A somewhat different case was recently considered theoretically [6]. The authors of ref. [6] studied numerically with both 1D GL equation and basic hydrodynamic equations Rayleigh-Benard (RB) convection subjected to a lateral throughflow. First, when a lateral flow is imposed in a long narrow channel heated from below, a stationary convection becomes an oscillatory one in a form of TW which propagates downstream. Its velocity grows with the throughflow velocity and thus can be varied externally. Secondly, due to zero value of the velocity imposed by the inlet boundary the TW

state is suppressed close to the inlet, and pushed further and further downstream at larger values of the axial flow. The distance of the TW state localization from the inlet l finally diverges at the critical value of the group velocity S^* which defines the transition from absolute to convective instability. Therefore at S^* convective rolls are «blown» out of the channel, and in the convectively unstable region one does not observe any pattern at all. Flow-induced propagating rolls exhibit a unique wave number selection [6]. Particularly surprising, one finds a complete absence of the stabilizing effect of the outlet sidewall, and the striking difference between the absence of flow patterns in the convectively unstable regime in this system and the rich variety of them in a closed convective system, *i.e.* downstream distance l approaches zero in a closed-flow system and infinity in the system considered, at the transition from the absolute to the convective instability regime. Here we would like to point out once more that the difference in the pattern behaviour is due to zero value of the velocity amplitude at the inlet boundary. In an infinite system similar pattern behaviour can be produced by suppressing the velocity amplitude somewhere in the interior of the system.

We expected that somewhat similar phenomena should be observed in a Couette-Taylor (CT) vortex flow subjected to an axial flow. On the other hand, the major difference between the RB and the CT systems in lateral boundary conditions may show up in this problem. Experimental evidence of the existence of propagating Taylor vortices with the superimposed throughflow was obtained in early studies [7]. Although various pattern selection and stability were the subject of the research [7], suppression of the Taylor vortex instability and existence of the oscillatory bifurcation were clearly demonstrated.

In this letter we concentrate on scaling properties and wave number selection of TW in the CT flow subjected to the axial flow in both convective and absolute instability regimes. Since there are no theoretical calculations for this specific system we compare our results with the theory developed for the RB convection with a lateral throughflow [6].

In the experiment we used a standard CT column installed horizontally and modified by an axial flow arrangement. The CT column and the superimposed throughflow are both temperature stabilized at the $\pm$ 10 mK level. Good temperature stabilization is a crucial part of the experiment due to substantial temperature dependence of the viscosity of the working fluid. As a working fluid a mixture of 32.4% by volume of glycerol in water at 22 °C ($\nu = 3.03cS$) was used. An axial flow was driven by gravity in a closed loop, and its average flow charge was measured by a precise flowmeter in the range from $2 \cdot 10^{-3}$ to 1.5 cm/s with a maximal resolution of $1 \cdot 10^{-4}$ cm/s. It was cross-checked by laser Doppler velocimetry (LDV) measurements in a Poiseuille flow regime before transition to TW. In order to make the axial flow as uniformly as possible in an azimuthal direction a stainless-steel net ((0.25×0.25) mm^2 mesh size) was used as nonrotating lateral boundaries on both sides of the column. Together with an inlet chamber and flow directors they produced a fairly homogeneous axial flow. Geometrical parameters of the column are: radius of inner cylinder is $R_1 = 1.900$ cm, radius of outer cylinder is $R_2 = 2.685$ cm (radius aspect ratio is 0.707), length aspect ratio is 27. Most of the measurements were performed by LDV, but visualization by adding 1% Kalliroscope was also used. In the latter case a video camera with a frame grabber was used to perform an image analysis.

In fig. 1 we present for comparison two sets of measurements: the open squares represent the experimentally determined velocity amplitude of the stationary Taylor vortices (without an axial flow), and the solid squares are the measurements of the velocity amplitude of TW near the outlet in the presence of the axial flow at Reynolds number $Re = \bar{v}d/\nu = 1.25$ both as a function of the control parameter ε. ($\bar{v}$ is the average velocity of the axial flow, $d = R_2 - R_1$, $\varepsilon = (T - T_c(Re))/(T_c(Re))$, $T = (4\eta^2 d^4)/(1 - \eta^2)(\Omega/\nu)^2$, $\eta = R_1/R_2$.) (ε here corresponds to μ in ref. [6].)

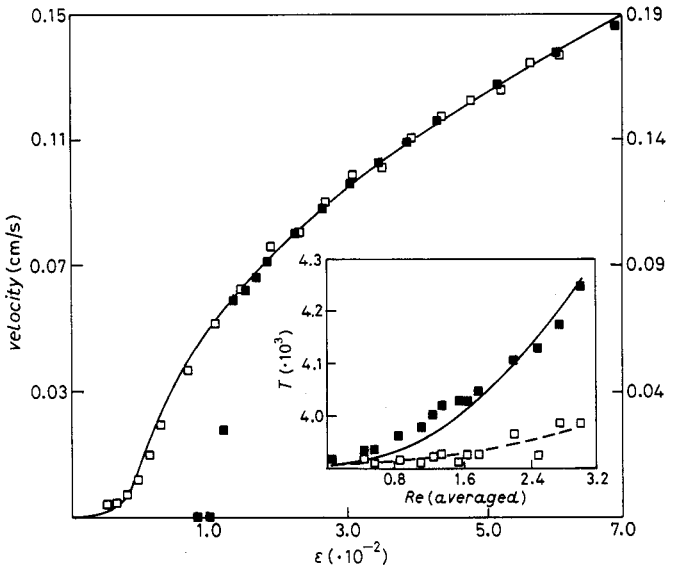

Fig. 1. – Amplitude of axial velocity *vs.* ε for two sets of data: open squares without throughflow, and solid squares for $Re = 1.25$ (velocity values on the left and right sides, respectively). Insert: stability diagram of CT flow with axial flow. Open squares are convective instability, solid squares are absolute instability limit. They are obtained from plots in fig. 1 (see text).

A fit by the amplitude equation gives the critical value of the Taylor number T_c which should correspond to the neutral line obtained by the linear stability analysis. Data for the velocity amplitude as a function of ε at $Re = 1.25$ exhibits its typical behaviour at $Re \neq 0$. The sudden fall of the velocity amplitude at $\varepsilon \simeq 0.01$ reflects the fact of expelling TW out of the system (fig. 1). Thus, this value of $\varepsilon(Re)$ should be close to the transition value from the absolute to convective instability $\varepsilon_{conv}(Re)$. Therefore, by performing measurements of the velocity amplitude as a function of T at the fixed values of Re one can reproduce both the convective and absolute instability lines for the CT flow subjected to the axial flow. These results are presented on the insert of fig. 1. Relatively large scatter of the experimental data for the convective instability line at larger Re is explained by the fitting procedure: at larger values of Re the data should be extrapolated far away to get $\varepsilon_c(Re)$. Both stability boundaries can be fitted by parabolic curves, respectively: $T_c(Re) - T_c(O) = aRe^2$, $a = 12.2$ for convective and $a = 58.3$ for absolute boundaries (broken and solid curves, respectively). The functional dependence is a direct manifestation of symmetry, but the coefficient value cannot be obtained from linear stability analysis [8*a*] as pointed out already in ref. [8*b*]. We emphasize here that no pattern is observed between these two lines. We can compare the absolute instability boundary with the theoretical criterion suggested in ref. [6] $\varepsilon(Re)_{conv} = \tau_0^2 S^2/[4\xi_0^2(1 + c_1^2)]$, where τ_0, ξ_0, S and c_1 are the coefficients of the GL equation (S denotes the group velocity). In the range $0 < \varepsilon < \varepsilon_{conv}$ TW are carried away from the system by axial flow. At $\varepsilon > \varepsilon_{conv}(Re)$ the CT flow becomes absolutely unstable, and the pattern can grow and expand upstream when the control parameter increases until TW fill the system completely. Figure 2 presents the experimental result together with the theoretical curve where we use values for τ_0 and ξ_0 from ref. [9], and we also use the fact that for the RB convection $S \simeq V_{ph}$ and c_1^2 is extremely small. Both approximations are definitely inside the error bars. V_{ph}, the phase velocity, was defined experimentally by tracing the wave front at successive times using a video camera and an image processing card, and was found to be $V_{ph} = 1.055\overline{v}$. From fig. 2 one concludes that experimental data are described

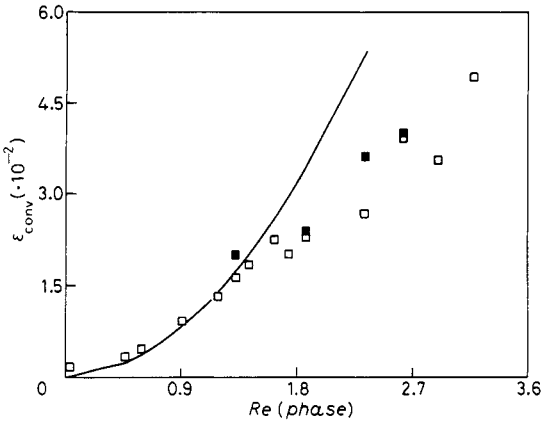

Fig. 2.

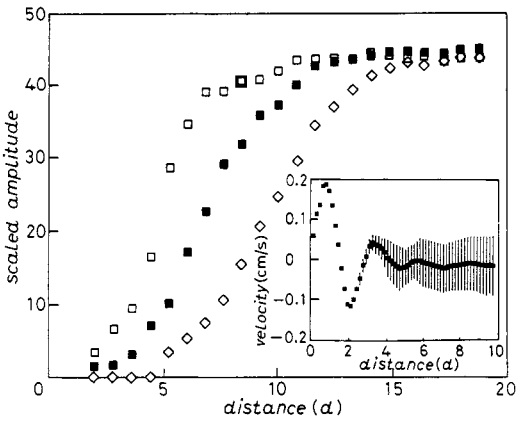

Fig. 3.

Fig. 2. – Stability diagram of CT flow in ε *vs.* Re coordinates (Re is calculated from V_{ph}). Solid curve is the theoretical curve (ref. [6]).

Fig. 3. – Profiles of TW velocities $(A(\tau_0/\xi_0)/\sqrt{\varepsilon})$ *vs.* distance from the inlet in units of d at $Re = 1.77$: open squares: $\varepsilon = 0.042$, solid squares: $\varepsilon = 0.034$, diamonds: $\varepsilon = 0.03$. Insert: the time-averaged axial velocity component (squares) and the velocity amplitude of the propagating Taylor vortices (bars) *vs.* distance from the inlet for $Re = 0.45$ and $\varepsilon = 0.012$ (measured at $0.2d$ from the inner cylinder).

fairly well by the theory up to $Re \simeq 1.35$, but then strongly deviate from the theoretical curve into the region of larger Re. Two sets of points are plotted: one set (open squares) was obtained from the solid squares in the insert of fig. 1, and the second one (solid squares) was obtained by measuring the distance from the inlet l and extrapolating it to infinity, at fixed ε. Both sets of data agree well. At $Re \geq 4$ one observes the spiral pattern at the absolute instability line but we will not discuss this pattern in this letter.

At the absolute instability boundary the growth rate of a localized perturbation is just equal to the downstream drift due to axial flow. At smaller velocity the pattern can expand toward the inlet into the interior of the system. Then TW produces a stationary amplitude profile whose distance from the inlet l decreases, while the control parameter ε increases until the pattern fills the system completely. This statement is illustrated in fig. 3 where the scaled envelope of TW velocity (amplitudes are scaled with $\varepsilon^{1/2}$) is plotted as a function of distance from the inlet for different values of ε and at fixed $Re = 1.77$. We would like to point out here that the velocity amplitudes, presented in fig. 1 and 3, are just related to the time periodic signal measured by LDV. Particularly close to the inlet and outlet this time modulation is observed on top of the regular Ekman vortices which exist near the lateral boundaries in a CT flow (see the insert in fig. 3). The detailed studies [10] show that the Ekman vortices are almost not influenced by the Poiseuille flow, while the amplitude of TW reaches zero at the lateral boundaries. This fact, probably, explains the similarity in RB and CT behaviour. A general scaling of $l_s = \varepsilon^{1/2} l/\xi_0$ at different values of $S_s = S(\tau_0/\xi_0)[\varepsilon(1 + c_1^2)]^{-1/2}$ was suggested and verified numerically in ref. [6]. Figure 4 presents all experimental data for the scaled length l_s *vs.* the scaled group velocity S_s. One finds two different parts of this curve. At $S_s < 2$ the scaled length l_s increases with S_s and at the transition line $S_s^* = 2$ probably diverges. The corresponding fit gives $l_s = 1.19(S_s^* - S_s)^{-0.6}$ (solid line). These data belong to $Re \leqslant 1.35$ which in fig. 2 are described well by the suggested criterion for the transition from the convective to absolute instability. The rest of the data at $Re > 1.35$ do

not satisfy the criterion, and one finds finite values of l_s at $S_s > 2$. The fit of these data gives $l_s = 2.26(2.71 - S_s)^{-1.46}$ (broken line). Thus this plot indicates the same discrepancy with the theory [6] which was already demonstrated in fig. 2.

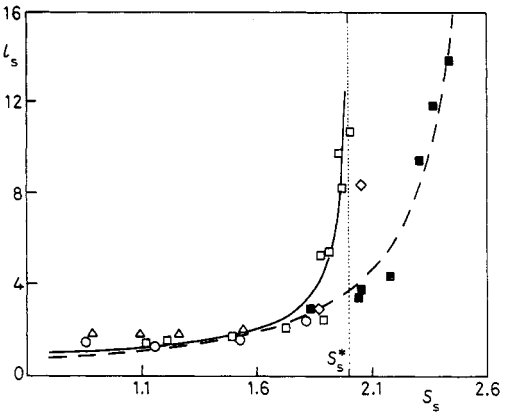

Fig. 4.

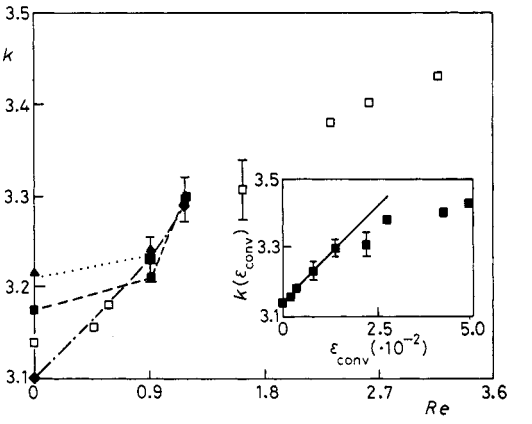

Fig. 5.

Fig. 4. – Scaled distance l_s *vs.* scaled group velocity S_s. Open squares: $Re = 1.25$, diamonds: $Re = 1$, triangles: $Re = 0.86$, circles: $Re = 0.56$, solid squares: $Re = 1.77$. Solid and broken lines are fit to the data (see text).

Fig. 5. – Wave numbers k *vs.* Re. Representative error bars are shown. Different symbols (diamonds, triangles, solid and open squares) correspond to different initial states prepared with different k at $Re = 0$. (Open square at $Re = 0$ corresponds to k_c.) Dash-dotted, dotted and broken lines show consequent k selected in the presence of flow with corresponding values of Re. Insert: wave number $k(\varepsilon_{conv})$ *vs.* ε_{conv}. The solid line is a fit to the part of the data below $Re \leqslant 1.25$.

The wave number selection of TW as a function of Re is demonstrated in fig. 5. We find that the bulk wavelength is independent of initial value of k prepared at $Re = 0$, hence the axial flow uniquely selects the wavelength. As seen from the plot in fig. 5, k increases with Re analogous to the theoretical predictions for RB convection with throughflow [6]. Nevertheless we did not observe the dependence of k on ε within our resolution in the range of the control parameters studied. In the insert of fig. 5 we present also the asymptotic values of the wave number on the boundary line between the absolute and convective instability regimes. We would expect that the wave number selection on the transition line $S_s^* = 2$ should be similar to the selection behind the propagating front [3, 11]. The corresponding selection behind the front of propagating waves was calculated [3] and at small values of c_1 and c_2 holds $k(\varepsilon_{conv}) - k_c \approx (c_1 + c_2)\,\varepsilon^{1/2}/2\xi_0$, where c_1 and c_2 are coefficients in GL equations [6]. Since according to ref. [6] $c_1 + c_2 = nRe$, one can fit the data in the insert of fig. 5 by $k - k_c = n(\varepsilon/\tau_0)$. The fit gives $n = 0.87$ at $Re \leqslant 1.25$, whereas for the convection flow n is at least an order of magnitude less [6].

* * *

The support of the Minerva Foundation and BSF US-Israel grant no. 8700406 is gratefully acknowledged. We acknowledge also useful and helpful discussions with M. LÜCKE.

REFERENCES

[1] See, *e.g.*, DOOLEN G., ECKE R., HOLM D. and STEINBERG V. (Editors), *Advances in Fluid Turbulence* (North-Holland, Amsterdam) 1989.
[2] LIFSHITZ E. M. and PITAEVSKI L. P., *Physical Kinetics* (Pergamon Press, New York, N.Y.) 1981, p. 268.
[3] NOZAKI K. and BEKKI N., *Phys. Rev. Lett.*, **51** (1983) 2171; DEISSLER R. J., *Physica D*, **25** (1987) 233; TAGG R., EDWARDS W. S. and SWINNEY H. L., *Phys. Rev. A*, **42** (1990) 831.
[4] CROSS M. C., *Phys. Rev. Lett.*, **57** (1986) 2935; *Phys. Rev. A*, **38** (1988) 3593.
[5] See, *e.g.*, STEINBERG V. *et al.*, p. 359; KOLODNER P. *et al.*, p. 319; CROQUETTE V. *et al.*, p. 300, in ref. [1].
[6] MÜLLER H. W., LÜCKE M. and KAMPS M., *Europhys. Lett.*, **10** (1989) 451.
[7] SNYDER H. A., *Proc. R. Soc. London, Ser. A*, **265** (1962) 198; BÜHLER K., *ZAMM*, **64** (1984) 180.
[8] *a*) CHANDRASEKHAR S., *Proc. R. Soc. London, Ser. A*, **265** (1962) 188; *b*) BÜHLER K., *Strömungsmechanik and Strömungsmachinen*, **34** (1984) 67.
[9] DOMINGUEZ-LERMA M. A., AHLERS G. and CANNELL D. S., *Phys. Fluids*, **27** (1984) 856.
[10] TSAMERET T. and STEINBERG V., to be published.
[11] FINEBERG J. and STEINBERG V., *Phys. Rev. Lett.*, **58** (1987) 1332; FINEBERG J., MOSES E. and STEINBERG V., *Phys. Rev. A*, **38** (1988) 4939.